

# Scanning Microscopy

---

Volume 10 | Number 4

Article 8

---

11-15-1996

## The Chromatin Structure of Well-Spread Demembrated Human Sperm Nuclei Revealed by Atomic Force Microscopy

M. J. Allen

*Digital Instruments, Inc.*, [mallen@di.com](mailto:mallen@di.com)


E. M. Bradbury

*University of California, Davis*

R. Balhorn

*Lawrence Livermore National Laboratory*

Follow this and additional works at: <https://digitalcommons.usu.edu/microscopy>

 Part of the [Biology Commons](#)

---

### Recommended Citation

Allen, M. J.; Bradbury, E. M.; and Balhorn, R. (1996) "The Chromatin Structure of Well-Spread Demembrated Human Sperm Nuclei Revealed by Atomic Force Microscopy," *Scanning Microscopy*. Vol. 10 : No. 4 , Article 8.

Available at: <https://digitalcommons.usu.edu/microscopy/vol10/iss4/8>

This Article is brought to you for free and open access by the Western Dairy Center at DigitalCommons@USU. It has been accepted for inclusion in Scanning Microscopy by an authorized administrator of DigitalCommons@USU. For more information, please contact [digitalcommons@usu.edu](mailto:digitalcommons@usu.edu).



## THE CHROMATIN STRUCTURE OF WELL-SPREAD DEMEMBRANATED HUMAN SPERM NUCLEI REVEALED BY ATOMIC FORCE MICROSCOPY

M.J. Allen<sup>1,\*</sup>, E.M. Bradbury<sup>2,3</sup>, R Balhorn<sup>4</sup>

<sup>1</sup>Digital Instruments, Inc., 112 Robin Hill Road, Santa Barbara, CA 93117

<sup>2</sup>Dept. Biol. Chem., Univ. Calif., Davis, CA 95616; <sup>3</sup>Life Sci. Div., Los Alamos Natl. Lab., NM 87545

<sup>4</sup>Biology and Biotechnology Research Program, Lawrence Livermore National Lab., Livermore, CA 94550

(Received for publication May 13, 1996 and in revised form November 15, 1996)

### Abstract

The fundamental structure formed when genomic DNA is packaged by protamine in the human sperm nucleus still remains essentially unresolved. It is known that the binding of protamine, a small arginine-rich protein, to DNA generates a large dense, hydrophobic complex making the sperm chromatin structure difficult to study microscopically. To visualize the internal nuclear structures, isolated human sperm nuclei were swollen extensively in saline buffer using only a reducing agent. The nuclei were swollen during deposition onto coverglass and then imaged in the atomic force microscope (AFM). The two main results obtained from imaging individual well-spread nuclei indicate that native human sperm chromatin is: (1) particulate, consisting primarily of large nodular structures averaging 98 nm in diameter, and (2) also composed of smaller, nucleosome-like particles observed to form linear chains near the nuclear periphery. These two types of chromatin particles imaged by AFM are remarkably similar to other AFM measurements made on native and reconstituted sperm and somatic chromatin.

**Key Words:** Sperm, chromatin, atomic force microscopy.

\*Address for correspondence:

Michael J. Allen  
Digital Instruments, Inc.  
112 Robin Hill Road  
Santa Barbara, CA 93117

Telephone number (805) 967-1400

FAX number (805) 967-7717

E-mail: mallen@di.com

### Introduction

Recent atomic force microscopy (AFM) studies of bovine sperm cell structures (Allen *et al.*, 1995) and various chromatin preparations (Allen *et al.*, 1993a, 1994; Leuba *et al.*, 1994; Martin *et al.*, 1995) have shown that these biological structures are preserved accurately using simple AFM sample preparations, even following air drying. The overall size and shape of the well-described nucleosome structure, as one example, is clearly resolved by AFM on reconstituted (Allen *et al.*, 1993a) and native (Allen *et al.*, 1994; Leuba *et al.*, 1994; Martin *et al.*, 1995; Yang *et al.*, 1994) chromatin fibers following air-drying of fixed and unfixed samples onto mica and coverslip glass. In some cases, the level of AFM resolution rivals and may exceed that of the electron microscope (EM).

In past studies, we have utilized AFM to obtain topographic images of the surfaces of condensed bull, mouse and rat sperm chromatin, nanodissected bull sperm chromatin and partially decondensed mouse sperm chromatin (Allen *et al.*, 1993b). These images show that the sperm chromatin in all four species is organized into tightly packed, large nodular structures approximately 50-100 nm in diameter. The nodular structures most likely represent a discrete sperm chromatin subunit similar in size to the spherical structures reported previously in numerous EM studies (Evenson *et al.*, 1978; Koehler, 1966, 1970; Koehler *et al.*, 1983; Tanphaichitr *et al.*, 1981) and in AFM/EM studies using reconstituted samples (Hud *et al.*, 1993).

Here, we report AFM images of chromatin structures imaged *in situ* on isolated and swollen human sperm nuclei adsorbed to coverglass. The AFM results indicate that chromatin in human sperm is entirely particulate and that the majority of the chromatin consists of particles many times the diameter of nucleosomes. This finding is consistent with a number of previous EM studies on intact and detergent-decondensed human sperm chromatin (Holstein and Roosen-Runge, 1981; Evenson *et al.*, 1978) and inconsistent with other EM findings that suggested either a smooth fibrillar or

nucleosomal organization (Gusse and Chevaillier, 1980; Sobhon *et al.*, 1982; Wagner and Yun, 1979). The same well-spread nuclei within which we observed the large chromatin particles, also exhibited smaller chromatin particles 45 nm in diameter suggesting the presence of nucleosomes in addition to the larger nucleoprotamine structures.

### Material and Methods

#### Preparation and isolation of amembraneous human sperm nuclei

Human sperm were obtained directly from semen. The semen was diluted with tris-saline (T/S) (150 mM NaCl, 10 mM Tris, pH 7.4), sonicated, and washed 3 times in 5 ml T/S (with centrifugation at 8,000 rpm for 4 minutes). The final pellet was resuspended in 4 ml of T/S to which 10 mg dithiothreitol (DTT) was added. This suspension was incubated on ice for 15 minutes. One ml of 5% mixed alkyltrimethylammonium bromide (MTAB) stock solution was added and mixed without sonication. This solution was incubated on ice for 1 hour with frequent mixing (not vortexing). The suspension was subsequently centrifuged at 5,000 rpm for 4 minutes and the pellet was then resuspended in T/S. This centrifugation and resuspension step was repeated 3 times. During the procedure sperm tails are detached during sonication and partially dissolve in MTAB along with other extra nuclear materials (Balhorn *et al.*, 1977). Demebrated sperm heads are separated from the debris during centrifugation.

#### Decondensation of amembraneous human sperm nuclei

Following MTAB treatment, human sperm nuclei were resuspended in 4 ml T/S and used immediately for decondensation. The timing of their use was found to be critical, because nuclear swelling did not occur if the suspension was allowed to sit more than an hour following MTAB treatment. Ten microliters of the amembraneous nuclei suspension was added to a 10  $\mu$ l droplet containing 8% beta-mercaptoethanol (BME; Sigma, St. Louis, MO) in distilled water which had previously been applied to a clean 15 mm round coverglass. The sperm suspension: BME mixture was then allowed to incubate on the glass for 4-6 hours at room temperature. The coverglass supporting the sperm droplet was placed in a humid chamber during the incubation to prevent dehydration. After incubation, the sample was rinsed with 50 drops of distilled water, wicked dry with tissue and placed in a vacuum desiccator chamber prior to imaging.

#### AFM Imaging of amembraneous sperm nuclei

The coverslips carrying the sperm chromatin (amembraneous nuclei) were scanned in air at 45% relative humidity at room temperature using a Nanoscope II

AFM (Digital Instruments, Santa Barbara, CA) in the contact scanning mode. The "height" or constant force mode was used and scan frequencies were typically 5 Hz. In order to minimize the force exerted by the AFM tip on soft samples, the set-point deflection was set at a value just above tip pull-off. In addition, AFM probes that exhibit very low adhesion with the substrate, as seen in "force versus distance plots," were chosen for imaging since they appeared to provide higher lateral resolution. Integral and proportional gain settings were raised until periodic noise could be seen in the AFM image or in "Scope Mode," the gains were then lowered until the noise completely disappeared. Typical settings were 6-8 and 9-12 for integral and proportional gains, respectively. All images presented are raw data (other than for "flattening" when needed) and are 400 x 400 data points. The images were rendered using a Nanoscope III offline workstation (Digital Instruments). Single-arm, 450  $\mu$ m long, etched silicon AFM probes with 5-10 nm end radii were used (provided by Digital Instruments). The "J" piezoelectric-tube scanner used was initially calibrated by Digital Instruments. The scanner was then routinely calibrated (approximately once per month) using various carbon, gold and silicon gratings with periods ranging from 0.463 to 10  $\mu$ m.

#### Fluorescence confocal microscopy of decondensed human sperm nuclei

Five microliters of propidium iodide (PI) in aqueous mounting media was applied to the glass coverslips supporting the decondensed amembraneous human sperm nuclei. The coverslips were then attached to clean microscope slides and additional coverslips were placed on top of the coverslips carrying the stained nuclei. The samples were then imaged with a Zeiss (Oberkochen, Germany) upright microscope using a 60 x, 1.4 numerical aperture (NA) oil objective. An integrated MRC-600 BioRad (Hercules, CA) argon laser scanning confocal microscope (LSCM) was used to excite the fluorochrome using the 514 nm line and detect red fluorescence using a photomultiplier tube. The areas on the coverslips that had previously been imaged by AFM were circled on the back side of the coverslip using a permanent ink pen at the time of AFM imaging. The microscope objective was positioned directly above these markings to facilitate locating the nuclei imaged previously by AFM.

### Results and Discussion

The chromatin spreading method described in this paper allows for the swelling of human sperm nuclei using the reducing agent beta-mercaptoethanol. In past studies of human sperm chromatin, high concentrations of salt, urea and nuclease were employed to facilitate decondensation and analysis by EM (Sobhon *et al.*, 1982;

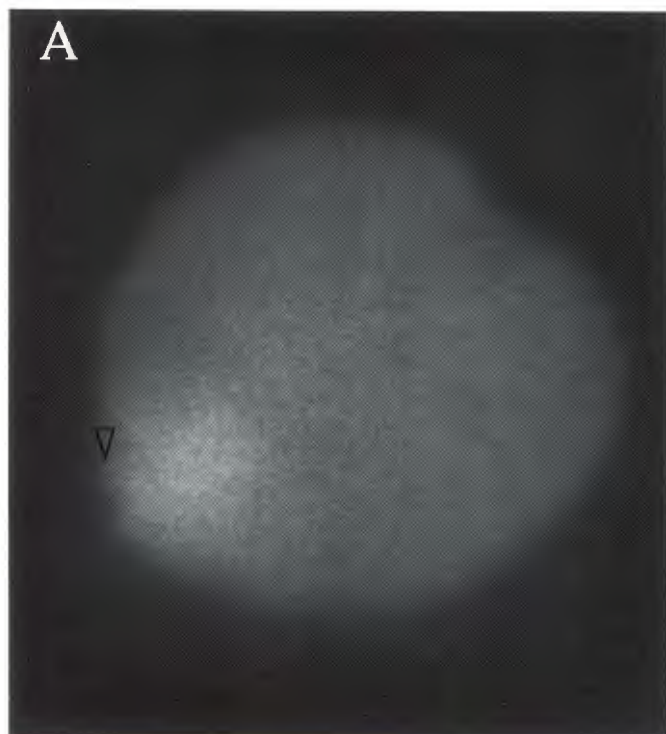
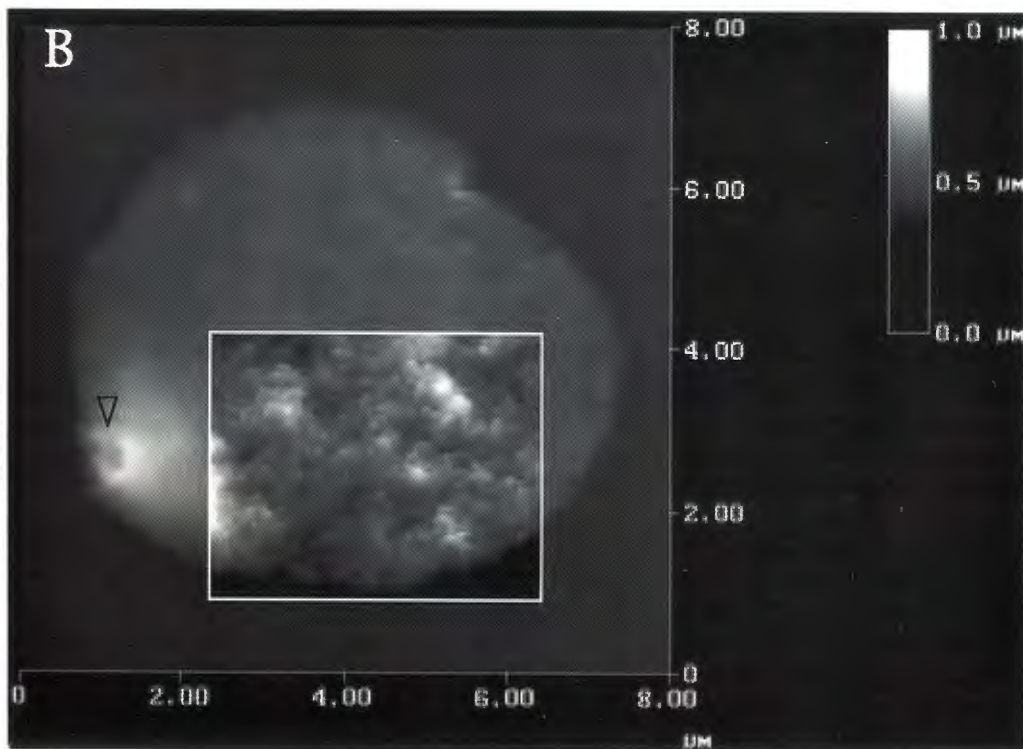


**Figure 1.** (A) LSCM and (B) AFM images of identical swollen human sperm nucleus. (A) Little detail is seen in the LSCM which detects the local intensity variations of the DNA stain (propidium iodide) excited by the scanning laser beam. (B) AFM detects the local height variations of the chromatin using a 5-10 nm radius contact probe-tip (fine topographic detail is seen in the inset). The arrowheads point out a region containing a circular structure detected by AFM commonly observed near an outer edge of swollen nuclei. Inset (in B) is a higher data-point resolution image (real-time zoom) showing fine detail of chromatin at the same area and x-y scaling as the overall image.



Tanphaichitr *et al.*, 1981). The present method, adapted from Wagner and Yun (1979), for our purposes, is desirable over other approaches since: (1) retention of isolated, individual nuclei is still possible after swelling, and (2) no protein loss is expected to occur during swelling minimizing perturbation of the chromatin structure.

As seen in Figure 1, LSCM (Fig. 1A) and AFM (Fig. 1B) images were obtained for identical human sperm nuclei swollen with reducing agent. The LSCM detects the local fluorescence intensity differences of the DNA staining pattern. Here, the two-point resolution is limited by approximately one-half the wavelength of the

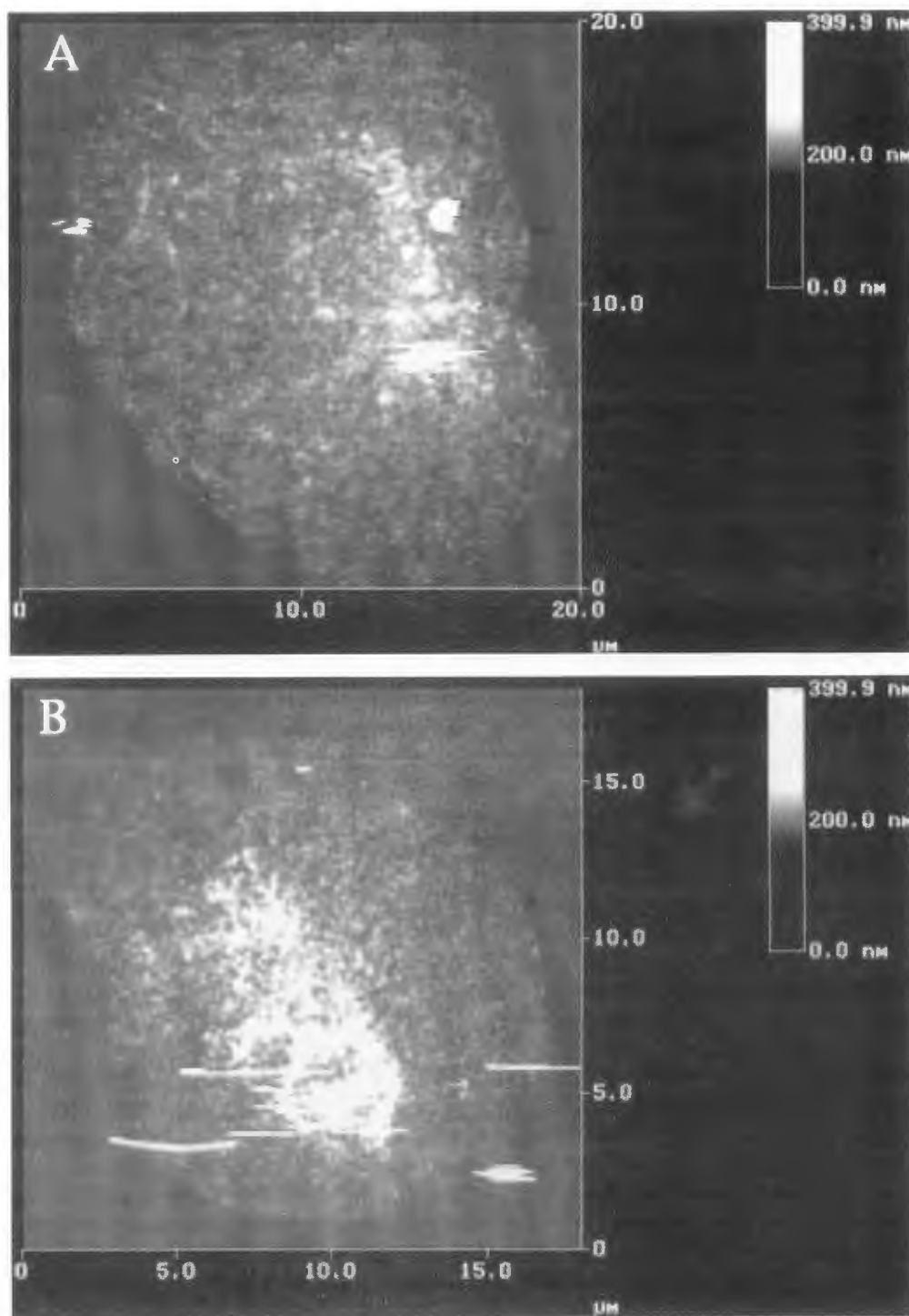


**Figure 2 (A and B).** Demembrated human sperm nuclei were swollen extensively by disrupting the protamine disulfide linkages with reducing agent. The normal pear-like shape was reduced to a highly flattened circular structure 15-20  $\mu\text{m}$  in diameter. Despite the great spreading, the nuclei retained a distinct outer perimeter locally intact at the chromatin edges.

fluorescent light emitted from DNA: PI complexes (700 nm). On the other hand, AFM detects the topographic surface properties of the sample with a contact probe 5-10 nm in radius of curvature. The inset in Figure 1B displays the fine topographic detail of the particulate chromatin detectable only by AFM. The arrowhead in Figure 1B points to a circular structure detected clearly by AFM at the outer edge of the chromatin surface.

This structure is similar in appearance to previous descriptions of an annular structure (Ward and Coffey, 1989) which participates in the anchoring of all 23 chromosomes in human sperm. The circular structure is just barely visible by LSCM (arrowhead in Fig. 1A) indicating that it is, at least partially, composed of DNA.

Amembraneous human sperm nuclei were swollen

## AFM of human sperm nuclei

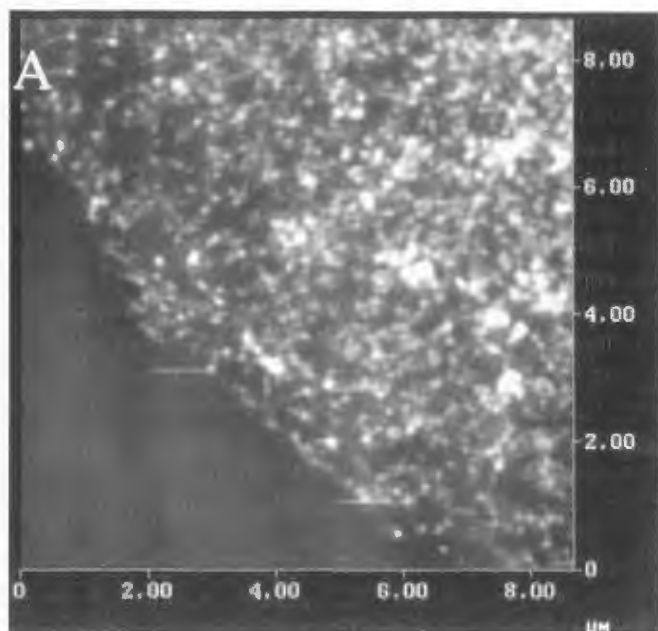
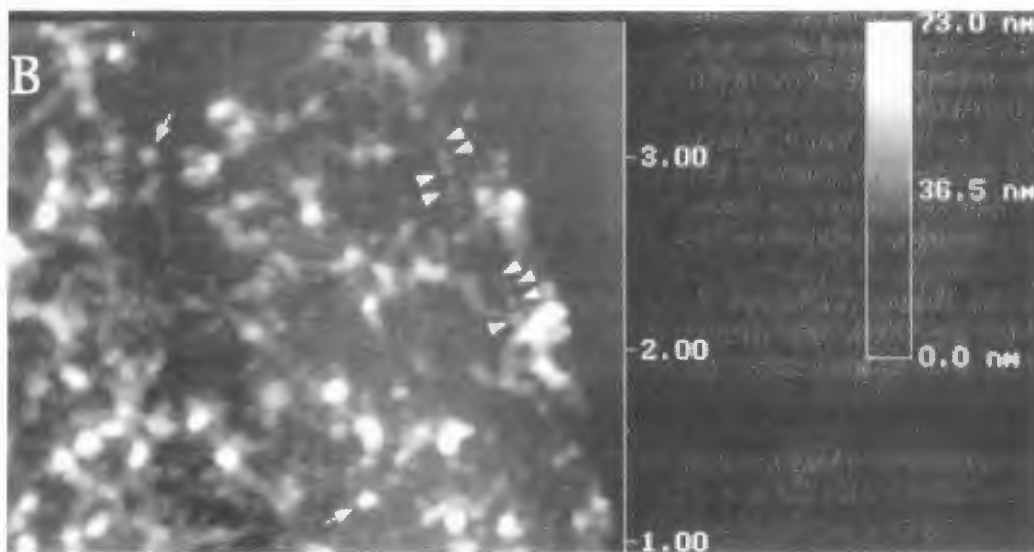


**Figure 3.** (A) Lower and (B) higher resolution AFM scans of human sperm chromatin spread onto coverglass as a thin chromatin layer. Nuclei remained isolated with clean edges following the spreading. (A) The sperm chromatin layer consists primarily of distinct nodular structures averaging 98 nm in outer diameter. (B) Near the perimeter of the nuclei, smaller nodular structures averaging 45 nm in outer diameter are clearly detected (arrowheads) in addition to the large nodes (arrows). In some cases, the smaller nodes were assembled into short linear chains (arrowheads). Units on X-Y axes is  $\mu\text{m}$ .



by reducing agent such that their normal pear-like shape and dimensions of  $5.5 \mu\text{m} \times 3.5 \mu\text{m}$  increased to a flattened circular shape  $15\text{-}20 \mu\text{m}$  in diameter (Fig. 2). The AFM images reveal that despite their great swelling, the nuclei retained a clean outer perimeter and appeared locally intact at the chromatin edges. The sperm chromatin layer consists primarily of distinct nodular structures  $97.7 \text{ nm} (\pm 11.2 \text{ nm})$  in outer diameter (Figs. 2 and 3; the well-spread nuclei shown in Figs. 2 and 3 are representative of the majority of nuclei on a particular coverslip prepared using the **Decondensation of amembraneous human sperm nuclei** method described in the previous section). However, nearer the perimeter of the nuclei, smaller nodular structures  $44.6 \text{ nm} (\pm 6.5 \text{ nm})$

in outer diameter are clearly detected (arrowheads in Fig. 3B) in addition to the large nodes (arrows in Fig. 3B). In some cases, the smaller nodes were assembled into short linear chains (arrowheads in Fig. 3B).

The AFM data for human sperm revealing the existence of small, linearly arrayed, nodular chromatin structures is consistent with the known presence of small quantities of core histone proteins in human sperm. The presence of all four core histones and the absence of histone H1 in human sperm has been established by both immunofluorescent and biochemical techniques (Gatewood *et al.*, 1990; Kolk *et al.*, 1976). Core histone octamers associated with sperm DNA would be expected to form nucleosomal bodies  $5.7 \text{ nm} \times 11 \text{ nm}$  in size

(Bradbury *et al.*, 1975). A lateral broadening effect, seen previously in AFM images of nucleosomal fibers caused by the finite AFM imaging probe, can account for nucleosomes appearing as large as 45 nm in the AFM image (Allen *et al.*, 1992). The dimensions and linear arrangements of the small nodular structures seen by AFM in decondensed human sperm chromatin are in good agreement with the AFM results we obtained on reconstituted H1-deficient nucleosome cores which measured up to 40 nm in diameter and assembled linearly along short DNA segments (Allen *et al.*, 1993a).

#### Acknowledgements

This work was performed at Lawrence Livermore National Laboratory under the auspices of the U.S. Department of Energy contract W-7405-ENG-48 to RB and grant DEFG03-88ER-60673 to EMB.

#### References

- Allen MJ, Hud N, Balooch M, Tench R, Siekhaus W, Balhorn R (1992) Tip-radius induced artifacts in AFM images of protamine-complexed DNA fibers. *Ultramicroscopy* **42-44**: 1095-1100.
- Allen MJ, Dong XF, O'Neill TE, Yau P, Kowalczykowski SC, Gatewood J, Balhorn R, Bradbury EM (1993a) AFM measurements of nucleosome cores assembled along defined DNA sequences. *Biochemistry* **32**: 8390-8396.
- Allen MJ, Lee C, Lee JD, Pogany GC, Balooch M, Siekhaus WJ, Balhorn R (1993b) Atomic force microscopy of mammalian sperm chromatin. *Chromosoma* **102**, 623-630.
- Allen MJ, Yau P, Bradbury EM (1994) Application of atomic force microscopy to the study of higher order chromatin structure. *Mol Biol Cell* **5**, 211a (abstract).
- Allen MJ, Bradbury EM, Balhorn R (1995) The natural subcellular surface structure of the bovine sperm cell. *J Struct Biol* **114**, 197-208.
- Balhorn R, Gledhill BL, Wyrobek AJ (1977) Mouse sperm chromatin proteins: Quantitative isolation and partial characterization. *Biochemistry* **16**: 4074-4080.
- Bradbury EM, Baldwin JP, Carpenter BG, Hjelm RP, Hancock R, Ibel K (1975) Neutron scattering studies of chromatin. *Brookhaven Symp Biol* **27**: 96-115.
- Evenson DP, Witkin SS, de Harven E, Bendich A (1978) Ultrastructure of partially decondensed human spermatozoal chromatin. *J Ultrastruct Res* **63**: 178-183.
- Gatewood JM, Cook GR, Balhorn R, Schmid CW, Bradbury EM (1990) Isolation of four core histones from human sperm chromatin representing a minor subset of somatic histones. *J Biol Chem* **265**: 20662-20666.
- Gusse M, Chevaillier Ph (1980) Electron microscope evidence for the presence of globular structures in different sperm chromatin. *J Cell Biol* **87**: 280-284.
- Holstein AF, Roosen-Runge EC (eds.) (1981) *Atlas of Human Spermatogenesis*. Electron Microscope Plates. Grosse Verlag, Berlin, Germany. pp. 110-115.
- Hud NV, Allen MJ, Downing K, Lee JD, Balhorn R (1993) Identification of the elemental packing unit of DNA in mammalian sperm cells by atomic force microscopy. *Biophys Biochem Res Comm* **193**: 1347-1354.
- Koehler JK (1966) Fine structure observations in frozen-etched bovine spermatozoa. *J Ultrastruct Res* **16**: 359-375.
- Koehler JK (1970) A freeze-etching study of rabbit spermatozoa with particular reference to head structures. *J Ultrastruct Res* **33**: 598-614.
- Koehler JK, Wurschmidt U, Larsen MP (1983) Nuclear and chromatin structure in rat spermatozoa. *Gamete Res* **8**: 357-370.
- Kolk AJ, Samuel T, Rumke P, Aarden LA, Bustin M (1976) Histone and DNA detection in swollen spermatozoa and somatic cells, by immunofluorescence. *Clin Exp Immunol* **24**: 63-71.
- Leuba SH, Yang G, Robert C, Samori B, van Holde K, Zlatanova J, Bustamante C (1994) Three-dimensional structure of extended chromatin fibers as revealed by tapping-mode scanning force microscopy. *Proc Natl Acad Sci USA* **91**: 11621-11625.
- Martin LD, Vesenska JP, Henderson E, Dobbs DL (1995) Visualization of nucleosomal substructure in native chromatin by atomic force microscopy. *Biochemistry* **34**: 4610-4616.
- Sobhon P, Chutatape C, Chalermisarachai P, Vongpayabal P, Tanphaichitr N (1982) Transmission and scanning electron microscopic studies of the human sperm chromatin decondensed by micrococcal nuclease and salt. *J Exp Zool* **221**: 61-79.
- Tanphaichitr N, Sobhon P, Chalermisarachai P, Patilantakarnkool M (1981) Acid-extracted nuclear proteins and ultrastructure of human sperm chromatin as revealed by differential extraction with urea, mercaptoethanol and salt. *Gamete Res* **4**: 297-315.
- Wagner TE, Yun JS (1979) Fine structure of human sperm chromatin. *Arch Androl* **2**: 291-294.
- Ward WS, Coffey DS (1989) Identification of a sperm nuclear annulus: A sperm DNA anchor. *Biol Reprod* **41**: 361-370.
- Yang G, Leuba SH, Bustamante C, Zlatanova J, van Holde K (1994) Role of linker histones in extended chromatin fibre structure. *Nature Struct Biol* **1**: 761-763.

#### Discussion with Reviewers

**B. Samori:** The swelling was carried out by a reducing agent, 2-mercaptoethanol which cleavages the disulfide

bonds. Therefore, the size of the particles should also depend on the primary structure of the packaging proteins. From this point of view, I am wondering that the distribution of the particle size is quite sharply peaked on two values, one the double of the other. Most likely, it has some meaning in terms of structure of sperm chromatin.

**Authors:** Two particle sizes are seen in the spread nuclei, 100 nm and 45 nm. In the intact demembrated nuclei, only 100 nm particles have been observed. Only when the nuclei are swollen, do we observe the smaller particles (at the nuclear periphery). Importantly, the large particles still far outnumber the smaller ones in the well-spread nuclei. Our interpretation of this is that the large particles do not reduce to two smaller particles during the 4-6 hour swelling with reducing agent. If this were true we would expect many more particles that are smaller than those observed on the intact nuclei.

**B. Samori:** Is the distribution of the sizes changing with 2-mercaptoethanol concentration or swelling time?

**Authors:** We have not looked at swelling as a function of reducing agent concentration. However, partially swollen nuclei resulting from shorter swelling times did not exhibit the smaller sized particles but these nuclei were not sufficiently spread to a monolayer to exclude the possibility that small particles exist buried in the nuclei and are not exposed at the surface.

**E. de Harven:** As stated by the authors (in describing Fig. 2), "the nuclei retained a clean outer perimeter and appeared locally intact at the chromatin edges." Can one exclude that the reason for this is not in the persistence of some components of the nuclear membrane or of the fibrous lamina? You constantly refer to these nuclei as "amembraneous," although you never demonstrate that they are effectively so. If this has been clearly demonstrated in one of your previous papers, this should be quoted to consolidate the notion that these isolated nuclei are indeed fully demembrated. Otherwise, an additional transmission electron microscope (TEM) thin section control of similarly prepared nuclei should be added to this paper.

**Authors:** Using TEM/thin sections, Balhorn *et al.* (1977) found no traces of extranuclear material on sperm nuclei that had undergone the same MTAB treatment as described in our current paper. While we are satisfied that little to no membrane is present on intact or swollen MTAB-treated sperm nuclei (also termed, chromatin particles), we feel, it is likely that other factors within the chromatin itself (e.g., a nuclear matrix) control nuclear architecture and help retain the clean outer perimeter observed in the well-spread nuclei.

**E. de Harven:** The attractiveness of the preparatory method used for your study is in its simplicity: the absence of chemical fixation, absence of critical point drying, etc. Still, have you observed with the AFM similarly prepared nuclei after fixation with glutaraldehyde or with other "EM-fixatives" and/or with critical point drying? Do you not think that this could facilitate the correlation between your observations and previous ultrastructural studies, well in the spirit of "correlative microscopy" which you already illustrate by applying both LSCM and AFM to the same nuclei? Please comment.

**Authors:** EM fixatives, metal coatings and other treatments allow accurate specimen preservation and good image contrast for this form of microscopy. As you point out, AFM does not require similar types of sample preparations. Recently, we performed a fairly extensive comparison between EM and AFM regarding preparation techniques for visualizing numerous substructures on bovine sperm cells (Allen *et al.*, 1995). The results clearly showed that, for the cellular substructures of bovine sperm, both EM and AFM sample preparation techniques, even though vastly different, gave nearly identical results. This was somewhat surprising since for AFM the cells were only air-dried or completely untreated (and imaged in buffer). In addition, we have imaged glutaraldehyde fixed nucleosomal fibers air-dried onto coverglass and were able to resolve clearly higher-order nucleosome packing and nucleosome core and linker DNA structures (Allen *et al.*, 1993a, 1994). These images suggested a good correlation of AFM to TEM metal-coatings on identical samples. We feel that EM and AFM provide inherently complementary information, and we foresee many more systematic studies that allow for even better correlation between imaging techniques, as suggested. However, our goals here were quite different. That is, we wanted to develop a technique for spreading the human sperm genome into a chromatin monolayer while retaining the integrity of individual nuclei we feel we have achieved this goal quite successfully and AFM was very helpful in analyzing the preparations and chromatin structures.

**J.K. Koehler:** Relative to the nuclear swelling treatments, you state "no protein loss is expected to occur ..." Has this actually been demonstrated experimentally?

**Authors:** Yes, although there is not a publication of ours that addresses this issue specifically, we have previously analyzed supernatants for protein content using gel electrophoresis and found no evidence of protamine or histone loss from the chromatin. So, we are fairly certain that there is little to no protein loss during MTAB and reducing agent treatment.



**J.K. Koehler:** The confocal image (Fig. 1A) appears to show a definite substructure consisting of short, worm-like segments, perhaps representing chromatin substructure. Could the authors comment on this?

**Authors:** There does appear to be some substructure in the confocal image shown in Figure 1A, however, we feel these subtle features are not well-resolved and are rather grainy in appearance causing us to question whether they are real. If in fact the nuclei consist entirely of closely packed particles no larger than 100 nm, as suggested by our AFM results, we would not expect to clearly resolve such structures using confocal microscopy on samples where the DNA is non-specifically stained. Generally, the confocal images show nuclei that appear uniformly stained with PI without any clearly discernible substructures.

**J.K. Koehler:** Can one obtain AFM images of normal, non-swollen sperm nuclei as a control? If so, what do they look like compared to the chemically treated nuclei?

**Authors:** Yes, we have imaged many intact human sperm nuclei and describe their appearance in the paper as "their normal pear-like shape and dimensions of 5.5  $\mu\text{m}$  X 3.5  $\mu\text{m}$ ." We have recently published more extensively on this subject (Lee *et al.*, 1996).

**J.K. Koehler:** Is there any suggestion of longer range, secondary order in the chromatin similar to the "plate-like" structures seen in early freeze-etch observations of non-human sperm?

**Authors:** We have seen no evidence of plate-like arrangements of the chromatin in intact or swollen human sperm nuclei. However, we would not necessarily expect to see these structures given our sample preparation for AFM. Such an arrangement might be observable by AFM by preparing and imaging thin sections of the nucleus. With regard to non-human sperm, we have seen limited evidence of plate-like arrangements in bovine sperm. In this case, using the AFM tip, we removed a layer of extranuclear material and exposed and imaged the chromatin layer below; this chromatin layer appeared to consist of 70 nm particles packed into a single plate-like structure.

#### Additional Reference

Lee JD, Allen MJ, Balhorn R (1996) Atomic force microscope analysis of chromatin volumes in human sperm with head-shape abnormalities. *Biol. Reprod* **56**: 42-49.